JOURNAL OF Materials CHEMISTRY

High surface area mesoporous titanium phosphate: synthesis and surface acidity determination

Deborah J. Jones,*[a] G. Aptel,[a] Markus Brandhorst,[a] Mélanie Jacquin,[a] José Jiménez-Jiménez,[b] Antonio Jiménez-López,[b] Pedro Maireles-Torres,[b] Ireneusz Piwonski,[a,c] Enrique Rodríguez-Castellón,[b] Jerzy Zajac[a] and Jacques Rozière[a]

[a]*Laboratoire des Agrégats Moléculaires et Matériaux Inorganiques, UMR CNRS 5072, Université Montpellier II, Place Eugène Bataillon, 34095 Montpellier cedex 5, France. E-mail: debtoja@univ-montp2.fr*
[b]*Departamento de Química Inorgánica, Cristalografía y Mineralogía, Universidad de Málaga, 29071 Málaga, Spain*
[c]*Department of Chemistry, University of Lodz, Pomorska 90236 Lodz, Poland*

Received 28th March 2000, Accepted 6th June 2000
Published on the Web 7th July 2000

A mesoporous form of titanium phosphate has been prepared by reaction between phosphoric acid solution and either titanium propoxide or titanium chloride in the presence of trimethylammonium surfactants. The surfactant can be almost completely removed by extraction using acidified ethanol. The surface area of the extracted samples depends closely on the pH of the reaction medium, and the reaction temperature, and the highest surface areas, around 740 $m^2\ g^{-1}$ were obtained for materials prepared at pH 3. This surface area is partially lost when the extracted titanium phosphate is calcined, although the mesoporous character is retained. ^{31}P NMR spectroscopy shows the ethanol-extracted sample to be rich in hydrogen phosphate (HPO_4^{2-} and $H_2PO_4^-$) groups, which undergo partial condensation after calcination. These hydrogen phosphate groups are responsible for the high surface acidity determined, and for its evolution after calcination: the total numbers of surface acidic sites of ethanol-extracted titanium phosphate and calcined titanium phosphate, evaluated using two-cycle adsorption of ammonia from the gas phase at 80 °C, are 900 and 340 μmol g^{-1} respectively.

Introduction

Several successful attempts have been made to synthesise mesostructured oxides other than those of silica and aluminosilicates using the supramolecular assembly approach developed by researchers at Mobil.[1] In particular, transition metals have properties appropriate for use in *e.g.* photoelectronics, catalysis or electromagnetics, which are not shown by aluminosilicates, and partial substitution of silicon by *e.g.* titanium,[2] vanadium,[3] iron,[4] manganese,[5] zirconium[6] and chromium[7] in MCM-41 type structures was rapidly achieved with the aim of conferring these properties on mesoporous matrices. In addition, several transition metal oxides, *e.g.* those of antimony, iron, molybdenum, tin, vanadium and chromium have also been prepared,[8–11] which show mesostructure in the presence of the templating surfactant molecules, although removal of the surfactant often leads to structure collapse. For non-silicic solids, conservation of a mesoporous structure after removal of the structure-directing agent still remains a challenge.[12] Important recent examples where the porous structure is retained include titanium[13–16] and zirconium[17–22] oxides. The key to the success of these syntheses was considered to lie in an increase of the degree of condensation, achieved either by the use of a surfactant with a phosphate head group, phosphate residues of which remain in the sample after calcination,[15,16,18] or stabilisation of the as-synthesised oxide by treatment with phosphoric acid.[13,17,19] Phosphorus-free mesoporous titanium oxide has been prepared using a dry aging technique,[20] and also by post-synthetic silanation.[23]

Porous hydrogenphosphates are a potentially important family of mesoporous materials since their high Brønsted acidity, coupled with high surface area and controlled pore dimension, will make of interest the investigation of acid catalytic activity. Titanium mesoporous materials are of considerable interest in the field of solid catalysed oxidation reactions. Layered titanium phosphate is precipitated by addition of a titanium(IV) or titanium(III) salt to aqueous phosphoric acid solution[24] and, depending on the concentration of phosphoric acid, structures of the type α-$Ti(HPO_4)_2H_2O$[25] or γ-$Ti(PO_4)(H_2PO_4).2H_2O$[26] of interlayer distance 7.8 and 12.4 Å respectively, are formed. The potentially high surface area provided by the layers is not, however, accessible unless these solids are pillared.[27] New types of titanium oxophosphates have recently been prepared,[28] as well as an open-framework templated structure $Ti^{III}Ti^{IV}(PO_4)(HPO_4)_2(H_2O)_2{\cdot}0.5NH_2(CH_2)_3NH_2$.[29] In addition, mesoporous vanadyl hydrogen phosphate has been prepared in a first study demonstrating[30] that the folding-sheet mechanism[31] type of synthesis route can be extended to non-silica mesoporous materials. In an alternative approach, it has been shown that calcination of zirconium phosphite benzene-1,4-diphosphonate leads to mesoporous zirconium phosphate pyrophosphate.[32] We have previously reported the synthesis of a mesoporous zirconium phosphate using a sol–gel synthesis method in the presence of a cationic surfactant,[33] and describe here the synthesis and characterisation of high surface area mesoporous titanium phosphate of high surface acidity using titanium chloride or titanium propoxide as sources of Ti(IV).

Experimental

Chemicals

Cationic surfactants $CH_3(CH_2)_nN(CH_3)_3Br$ with $n=7$, 11, 15 and 17, tetramethylammonium hydroxide (25 wt% solution in

water), orthophosphoric acid (85 wt%), titanium propoxide (98%) and titanium chloride were purchased from Aldrich. Ethanol (95%) and hydrochloric acid were Carlo Erba products. All chemicals were used as received.

Synthesis

Two synthesis methods were developed using the two different sources of titanium. For synthesis using titanium propoxide, the synthesis was carried out by mixing an aqueous solution (25 wt%) of surfactant $CH_3(CH_2)_nN(CH_3)_3Br$, $n=7$, 11, 15 and 17, with phosphoric acid to give a P/surfactant molar ratio of 1 at temperatures ranging from 50 to 75 °C. The acidified surfactant solution was then aged for at least 60 minutes, and the pH value adjusted to between pH 1 and pH 6 with tetramethylammonium hydroxide solution (diluted to 12.5 wt%). Titanium propoxide was added to this solution, to give a P/Ti mole ration of 1 or 2. A gel formed immediately, and this was either kept at the chosen temperature for 2 days, or subjected to mild hydrothermal treatment at 120 °C for 1 day. In each case the solid was then recovered by centrifugation and dried at 50 °C.

Various routes were investigated for removal of the surfactant template: solvent extraction in ethanol/HCl, solvent extraction followed by a calcination step, and direct calcination. For extraction, 0.6 g of the as-prepared sample was generally suspended, with stirring, in 50–200 cm^3 acidified ethanol solution. Ethanol was acidified with HCl in volume ratios of 100/1–10, and extraction times were varied from 30 min to 2 d. The extracted solid was then recovered by centrifugation and dried at 50 °C. Calcination was performed in air using a ramp rate of 2 °C min^{-1} up to 540 °C, followed by 4 h at this temperature.

For the synthesis using titanium chloride, equal volumes of an aqueous solution of $TiCl_4$ (1 mol dm^{-3}) and H_3PO_4 (2 mol dm^{-3}) were mixed, and then stirred either at room temperature for 24 h or maintained under reflux for 48 h. The solid titanium hydrogen phosphate produced was recovered by centrifugation, washed free of chloride ions with 2% H_3PO_4, excess phosphoric acid removed by extensive washing with deionized water, and the product dried in air at room temperature. X-Ray diffraction showed that the product formed at room temperature after 24 h was semi-amorphous, whilst that recovered after 48 h under reflux gave a diffraction pattern characteristic of α-titanium phosphate.[25] Tetramethylammonium hydroxide solution (25 wt%) was added to an aqueous suspension (typically 1.3 g in 10 cm^3 of deionized water) of these dense titanium phosphate phases to yield a basic (pH 11–14) solution. To this was added an aqueous solution of hexadecyltrimethylammonium bromide (25 wt%) (molar ratio C16TMA/phosphorus of 1) and the mixture was stirred for 3–5 h at 65 °C. The sol was then acidified to pH 1–5 with a 2 mol dm^{-3} solution of H_3PO_4, and the gel which was formed was stirred for 2 days at 65 °C, after which the solid phase was recovered by centrifugation and dried at 60 °C. The surfactant was removed by extraction with an ethanolic solution of HCl, followed by outgassing under vacuum at 250 °C and calcination at 400 or 540 °C.

Characterisation

Powder X-ray diffraction patterns were recorded using a Philips X-Pert instrument with Cu Kα radiation. Adsorption–desorption of nitrogen at 77 K was performed using a Carlo-Erba Sorptomatic series 1800 instrument, and the Brunauer–Emmett–Teller (BET) surface area determined. Pore diameters were estimated using the Cranston–Inkley method.[34] Thermogravimetric analyses were carried out using a Stanton-Redcroft STA-781 series thermal analyser under static air, with a heating rate of 1 °C min^{-1}. Infrared spectra were used, in conjunction with thermogravimetric data, to determine the extent of surfactant removal. FTIR spectra in the region 400–4000 cm^{-1} were recorded as KBr discs on a Bomem DA8 spectrometer. Transmission electron micrographs were obtained with a JEOL 1200 EX microscope operating at 100 kV. ^{31}P MAS NMR spectra were recorded using a Bruker 400 spectrometer. Determination of surface acidity was carried out by two-cycle adsorption of ammonia from the gaseous phase at 80 °C. The chemisorption of ammonia from the gas phase as a method of determining the surface acidity of MCM-41 type solids has been reported.[35] In the present study, the amounts of NH_3 adsorbed at different partial pressures in the equilibrium bulk phase were measured using a Micromeritics ASAP 2010 Chemi System apparatus. In order to reduce physisorption of ammonia on the solid surface, the adsorption temperature was maintained at 80 °C.

Prior to adsorption measurements, the sample (about 200 mg) was outgassed at 250 °C for 3 h. Successive ammonia doses were sent onto the sample until a final equilibrium pressure of 38 Torr was reached. The equilibrium pressure was measured after every adsorption step and the amount adsorbed was calculated. At the end of the first adsorption cycle, the sample was pumped at 80 °C for 30 min and a second adsorption cycle was then performed at the same temperature. The difference in adsorption between two adsorption cycles is ascribed to irreversible adsorption of NH_3 on surface of the titanium phosphate. At first, this quantity changes as the adsorption progresses, but then it levels off. Since irreversible adsorption of NH_3 means the localised chemisorption of single ammonia molecules on acidic sites, this quantity provides the total number of acidic sites on the solid surface.

The number and strength of surface acid sites were also evaluated by thermoprogrammed desorption of ammonia. The sample was pre-treated in a helium flow of 35 cm^3 min^{-1} at 550 °C for 1 h and then saturated in an ammonia flow of 70 cm^3 min^{-1} at 100 °C for 5 min. Helium carrier gas was subsequently flowed through the sample at the rate of 35 cm^3 min^{-1} and 100 °C until the NH_3 molecules physisorbed on the surface were completely removed, as indicated by an on-line gas chromatograph (Shimadzu GC-14A) equipped with a TC detector. Ammonia desorption betweeen 100 and 550 °C (heating rate 10 °C min^{-1}) was analysed with the same detector.

A flow-calorimetric study of the adsorption of gaseous ammonia at 80 °C was also carried out with the use of a 4Vms Microscal Flow Microcalorimeter[36] to evaluate the strength of surface acidic sites. This technique is based on a flow-injection adsorption procedure and involves injection of small amounts of ammonia into the stream of helium carrier gas percolating through the adsorbent in the calorimetric cell. It was designed for the determination of the heats of adsorption of irreversibly adsorbed ammonia at increasing degrees of surface coverage. Prior to measurement samples were out-gassed at 80 °C overnight, and then flushed with helium for 4 h. The downstream TC detector determines the concentration of that part of the injected ammonia in the effluent which is not retained by the titanium phosphate. The heat effect obtained as a result of the injection corresponds only to the irreversibly adsorbed ammonia. The relevant pseudo-differential molar heat of adsorption could be thus accurately measured for a given degree of surface coverage. The injections were continued until there was no more irreversible adsorption. At that point all the acidic sites on the mesoporous titanium phosphate were saturated and further adsorption was fully reversible. The number of injections to saturate the acidic surface was decided based on the results of the above ammonia adsorption study carried out under static conditions. The flow rate of helium was 1 ml min^{-1}.

Results and discussion

In initial experiments, reaction conditions described previously for the synthesis of mesoporous zirconium phosphate[33] were adopted, substituting titanium propoxide for zirconium isopropoxide. This direct transposition led to materials, after surfactant removal by solvent extraction, of surface area *ca.* 150 $m^2 g^{-1}$, significantly lower than that of the zirconium congener, which is around 330 $m^2 g^{-1}$. The reaction temperature and pH value of the reaction medium were therefore modified in attempts to obtain materials of higher surface area. In addition, the influences of surfactant chain length, phosphorus to titanium mole ratio, hydrothermal aging, extraction methods, and post-synthetic treatment on the formation of a mesoporous titanium phosphate were also studied.

Surfactant extraction

Fig. 1(a) shows the thermogravimetric curve for a titanium phosphate sample prepared using dodecyltrimethylammonium (C12TMA) bromide as the structure-directing agent, after warm-water washing and drying. A first plateau may be seen at 160–200 °C which corresponds to the end of water desorption, and the beginning of template decomposition and desorption. The weight loss between 150 and 500 °C then occurs in two steps, with a second plateau observable at 275 °C. The total weight loss of 38% that occurs in this range corresponds mainly to decomposition and elimination of the surfactant, but also to condensation of hydroxy groups. The TGA curve of Fig. 1(b) suggests the solvent extraction procedure to be efficient, since beyond the *ca.* 20% weight loss to 150–180 °C due to elimination of water and ethanol adsorbed during the extraction and washing steps, only a further *ca.* 8% loss occurs up to 500 °C, which includes the decomposition of residual surfactant and elimination of water produced by condensation of surface –OH groups. At higher temperatures, the differential thermal analysis of both as-prepared and extracted samples shows a futher exothermic effect at 750 °C, which is not associated with a weight loss, and which corresponds to a structural transition to, principally, $(TiO)_2P_2O_7$ and anatase, as identified by X-ray diffraction.

The influences of different HCl/ethanol concentrations, the solid/solvent ratio and the extraction time on the efficacy of surfactant extraction were studied, evaluated using the residual weight loss between 200–500 °C in TGA, and the intensity of vibrations in IR spectra arising from CH_2 and CH_3 stretching and bending vibrations, relative to those of the phosphate group. Fig. 2 shows the IR spectra of a templated TiP prepared using hexadecyltrimethylammonium bromide, and the same material after HCl/ethanol extraction and calcination. Extraction was performed at room temperature in a 2% v/v HCl/ethanol solution with a solid/solvent ratio of 0.6 g/100 cm^3 and

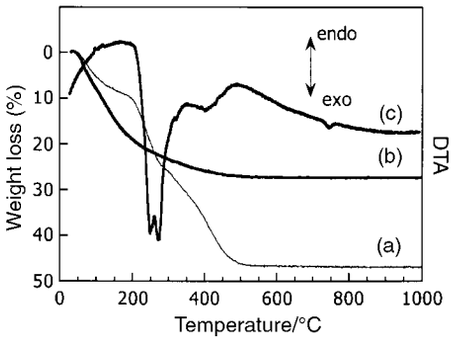

Fig. 1 Thermogravimetric analysis of (a) surfactant–titanium phosphate mesophase, (b) solvent-extracted titanium phosphate and (c) corresponding differential thermal analysis (titanium propoxide precursor).

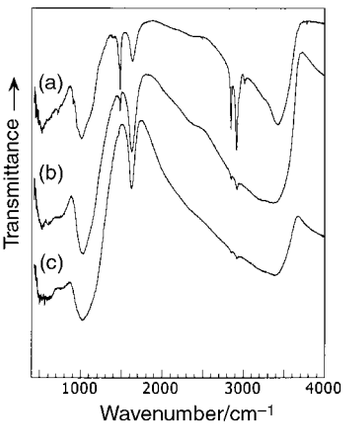

Fig. 2 Infrared spectra of (a) surfactant–titanium phosphate mesophase, (b) solvent-extracted and (c) solvent-extracted and calcined (540 °C) titanium phosphate (titanium propoxide precursor).

an extraction time of 2 h. The intensity of the absorptions in the IR spectrum due to the surfactant is significantly reduced in the extracted sample, and these peaks disappear after calcination. An increase in the volume of the solvent, lengthening of the duration of extraction or increase in temperature did not significantly reduce the amount of surfactant, as estimated from TGA and IR, but reducing any of these factors was found to lead to less complete surfactant removal. The above conditions were adopted in all further preparations.

The X-ray diffraction pattern of an as-prepared mesoporous titanium phosphate prepared using C16TMA is shown in Fig. 3. In the range up to 10° 2θ, 3 peaks are observed, the first of which is broad, with $d = ca.$ 45 nm. These could correspond to a layered arrangement, which would collapse after surfactant removal, but this is incompatible with the high surface area and mesoporosity observed for the present materials after solvent extraction and calcination. In addition, if these peaks were to be arbitrarily indexed to (100), (200) and (400) diffraction, observation of (300) would also generally be expected, which is not the case here. More probably, the diffraction pattern should be differently interpreted. Indeed, the breadth of the first peak may arise from superposition of several diffraction lines as would be expected for a disordered cubic-like structure. Transmission electron microscopy of the surfactant–titanium phosphate mesostructure also shows particular types of ordering, Fig. 4. Highly structured hexagonal ordering of the type characteristic of MCM-41 is not observed; rather, different structural features are seen: regions showing a disordered channel structure, of a uniform cross-sectional diameter, and regions which show more marked alignment of the pores. Furthermore, partial "finger-print" structures are visible, as shown also in zirconium oxide-sulfate[19] and MCM-41 materials,[37] which were identified[38] as

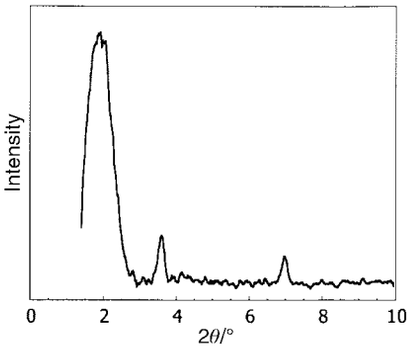

Fig. 3 X-Ray diffraction pattern of surfactant–titanium phosphate mesophase (titanium propoxide precursor).

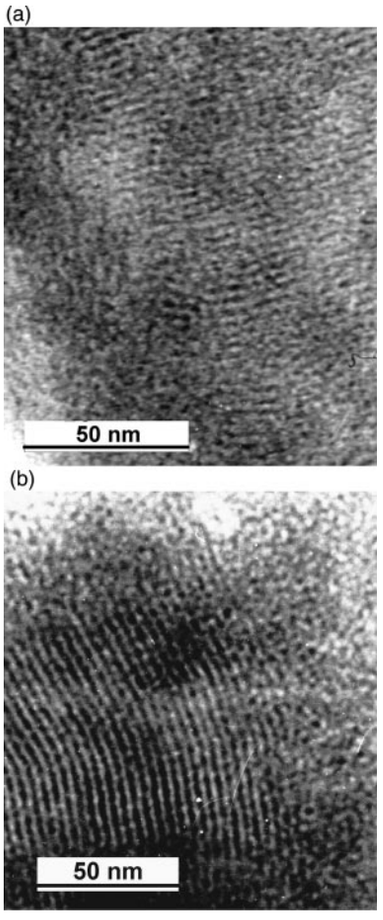

Fig. 4 Transmission electron micrographs of (a) surfactant–titanium phosphate mesophase from titanium propoxide precursor and (b) surfactant–titanium phosphate mesophase from $TiCl_4$ precursor.

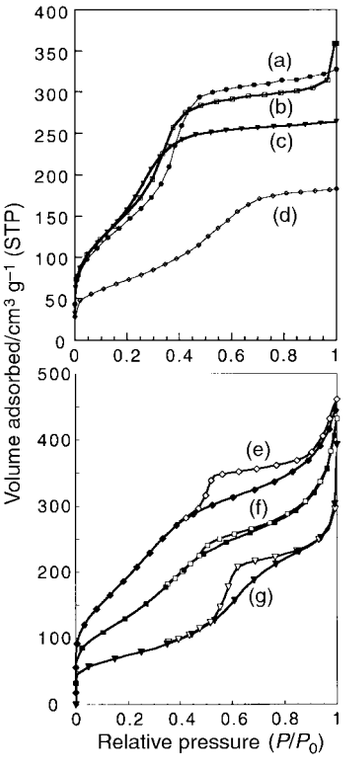

Fig. 5 (a)–(d) Nitrogen adsorption isotherms of solvent-extracted titanium phosphates (a) TiP7, (b) TiP6, (c) TiP8 and (d) solvent extracted and calcined (540 °C) TiP6 (see Table 1). The isotherms in (a)–(d) are reversible and only the adsorption branch is shown. (e)–(g) Nitrogen adsorption–desorption isotherms of (e) solvent-extracted TiP100, (f) as (e) calcined at 400 °C, (g) as (e) calcined at 540 °C.

disclination effects which are well known in liquid crystal systems.

Textural characteristics

Titanium phosphate samples prepared using titanium propoxide and using titanium chloride have different textural characteristics. The nitrogen adsorption–desorption isotherms at 77 K of TiP materials obtained using titanium alkoxide are of type IV and are fully reversible with no hysteresis, Fig. 5(a)–(c). They exhibit a sharp inflection characteristic of capillary condensation, and the verticality of the step in P/P_0 between 0.3 and 0.5 indicates a narrow pore size distribution. Table 1 summarises the textural parameters derived from the isotherms of extracted samples obtained under different reaction conditions, in particular pH, reaction temperature and surfactant chain length. The highest surface area materials, up to 650 $m^2\ g^{-1}$, were obtained when the pH of the reaction medium was between 3 and 4, and with a reaction temperature of 75 °C. Under otherwise identical reaction conditions, the pore volume is higher for titanium phosphates prepared with longer chain trimethylammonium surfactants (C16TMA, $V_p = 0.790\ cm^3\ g^{-1}$) than with C12 (0.406 $cm^3\ g^{-1}$) or C8 (0.283 $cm^3\ g^{-1}$). The application of Cranston and Inkley's cylindrical pore method[34] indicates the presence of a uniform pore size distribution, which is narrowest for the material obtained after 1 day of hydrothermal treatment at 120 °C of a templated titanium phosphate gel obtained at pH 3 and 75 °C. The use of a higher temperature or longer time leads to materials with lower surface area and less uniform pore size distribution. As observed for surfactant templated silica and heteroatom doped silica, and in contrast to certain mesoporous titania preparations,[20] the average pore size increases as the chain length of the surfactant increases. Extracted titanium phosphate samples prepared with C12TMA and C16TMA have pore diameters of 2.5 and 2.8–3.1 nm respectively. The surface areas shown by the extracted titanium phosphates described here lie in the range of those recently reported for mesoporous titania,[14,20] in which the surfactant was also removed by solvent extraction.

Direct calcination, or calcination of extracted samples to 540 °C, results in partial loss of surface area. Irrespective of the surface area of the extracted sample, all calcined samples have a similar surface area of about 250 $m^2\ g^{-1}$ and retain their mesoporous character. However, pore filling during adsorption occurs both at higher, and over a broader range of, relative pressures indicating a broader pore distribution of greater average pore diameter (Fig. 5(d)). In other mesoporous transition metal oxides, a similarly observed loss of surface area has been attributed to the possibility that the crystallisation of the corresponding dense oxide is already favourable at temperatures below that required for surfactant removal and condensation of –OH groups.[19] Schüth has reported stabilisation of mesoporous zirconia[17,19] and titania[13] by post-synthesis phosphoric acid treatment. In the present case, the material is already rich in phosphate groups and further phosphoric acid treatment of either as-synthesised or extracted samples gave no improvement in surface area after subsequent calcination.

To determine the temperature at which this loss of surface area begins, samples were calcined at 200 °C and 300 °C. Whereas the inital surface area of the extracted sample was maintained at 200 °C (698 $m^2\ g^{-1}$), at 300 °C significant loss has occurred (379 $m^2\ g^{-1}$). It is known from TGA and IR that only small amounts of surfactant remain after HCl/ethanol extraction but it is possible that this plays a stabilising role. It is more probable, however, that above 300 °C the surface hydroxy groups condense and this process may lead to partial sintering. However, a higher surface area is retained

Table 1 Textural parameters of mesoporous titanium phosphate: dependence of synthesis and surfactant removal conditions (samples TiP1–TiP9 synthesised using titanium propoxide; samples TiP100, TiP101 synthesised using $TiCl_4$)

Sample	Reaction temperature	pH of reaction medium	Surfactant chain length	BET surface area/$m^2\ g^{-1}$	V_p/$cm^3\ g^{-1}$	d_{pore}/nm
TiP1[a]	50	1	C16	271	0.372	—
TiP2[a]	50	3	C16	340	0.529	3.0
TiP3[a]	50	4	C16	336	0.230	—
TiP4[a]	50	6	C16	207	0.214	—
TiP5[a]	65	3.5	C16	456	0.356	3.0
TiP6[a]	75	3	C16	597	0.790	2.8
TiP7[b,a]	75	3	C16	521	0.498	3.1
TiP8[a]	75	3	C12	650	0.406	2.5
TiP9[a]	75	3	C8	398	0.283	—
TiP 6[c]	75	3	C16	260	0.285	4.2
TiP100[d]	65	3	C16	740	0.688	2.3
TiP101[e]	65	3	C16	615	0.416	2.8
TiP100[f]	65	3	C16	493	0.628	2.8
TiP100[d]	65	3	C16	291	0.524	5.1

[a]Extracted with HCl/ethanol. [b]Treated hydrothermally at 120 °C for 24 h. [c]Extracted with HCl/ethanol and then calcined at 540 °C. [d]Sample TiP100 prepared *via* semi-amorphous titanium phosphate precursor. [e]Sample TiP101 prepared *via* crystalline titanium phosphate. [f]Extracted with HCl/ethanol and then calcined at 400 °C.

after calcination than has been reported for mesoporous titanium oxides,[14,20] which confirms the reported stabilising influence of surface hydrogen phosphate groups.[13,19]

In the preparation route starting from titanium chloride, dense titanium phosphate is precipitated in a first step, which is redispersed in tetramethylammonium hydroxide and C16TMA solution. In experiments comparing the textural properties of the ultimate products, high surface area materials are obtained when the dense titanium phosphate precursor phase is either semi-amorphous or crystallised, layered α-titanium phosphate. Conversion of layered to mesoporous titanium phosphate may therefore occur *via* a "folded sheet" mechanism, as previously reported to take place with layered silicic acids[31] and vanadyl hydrogen phosphate.[30]

Textural characteristics of titanium phosphate prepared using titanium chloride are given in Table 1, and the corresponding adsorption–desorption isotherms in Fig. 5(e)–(g). These isotherms differ from those given by mesoporous titanium phosphate prepared using titanium propoxide, in that all show a hysteresis loop, and there is no pronounced step in the P/P_0 region of 0.2–0.4, which indicates a broader pore size distribution. Precipitation at pH 3 gives the material of highest surface area, 740 $m^2\ g^{-1}$, and on subsequent calcination at 400 and 540 °C partial loss of surface area occurs, to 493 and 291 $m^2\ g^{-1}$ respectively. The average pore size increases from 23 Å in the extracted material, to 28 Å on calcination at 400 °C, and then broadens after calcination at 540 °C, with an average pore diameter of 51 Å.

Spectroscopic characterisation

Elemental analysis of typical extracted samples gave a P/Ti ratio of 1.4 for materials prepared using $TiCl_4$ and 1 for materials prepared using titanium propoxide. For the latter, the addition of acetylacetone to the alkoxide to reduce the speed of its hydrolysis and condensation did not lead to a higher framework P/Ti ratio. ^{31}P NMR spectra of as-synthesised, extracted and calcined samples exhibit broad signals, as expected for phosphorus in a large range of environments. ^{31}P NMR data of various titanium phosphates and oxophosphates[28,39–43] have been reported. Studies of titanium phosphates of known crystal structure have shown a correlation between connectivity and chemical shift. As the connectivity increases, an upfield shift is observed from −5.3 to −10.6 ppm for H_2PO_4 to −18.1 ppm for HPO_4 and finally to −19 to −32.5 for PO_4.[28,39–42] In addition, deprotonation and/or hydrogen bond donation causes a downfield shift of approximately 1 to 10 ppm.[42] Hydrogen bonding also leads to broadening of the signal.[40] A comparison of the position of the signals obtained (Fig. 6) with the above reported data indicates that for the as-synthesised sample few phosphate groups with connectivity four are present. The ^{31}P signals for connectivity 1, 2 and 3 are at least partly shifted downfield due to deprotonation of hydrogen phosphate groups in the presence of cationic surfactant.[43] For the extracted and calcined samples, interaction with water (uptake of atmospheric water even by the calcined sample is rapid) takes place also causing a downfield shift.[39] A superposition of all three spectra shows a progressive upfield shift of the signal from the as-synthesised to the extracted to the calcined product. While the difference from the as-synthesised to the extracted product might be attributed to a change in the degree of protonation of P–OH groups, the shift from the extracted to the calcined product is most probably the result of an increase in connectivity. The strong absorption at 3360 cm^{-1} in the infrared spectrum of the extracted sample (3380 cm^{-1} in the calcined material) is due to the P–OH stretching mode.[44]

Surface acidity characteristics

Thermoprogrammed desorption of ammonia (NH_3 TPD) was used for the evaluation of the number of surface acid sites. The results of NH_3 TPD on a sample extracted with HCl/ethanol are shown in Fig. 7. The total acidity value is quite high, 711 μmol g^{-1}, with a broad distribution of acid strengths. Around 60% of the ammonia is desorbed between 100 and 300 °C, which reflects the predominance of surface POH and $P(OH)_2$ groups in this temperature range. However, Fig. 7 also

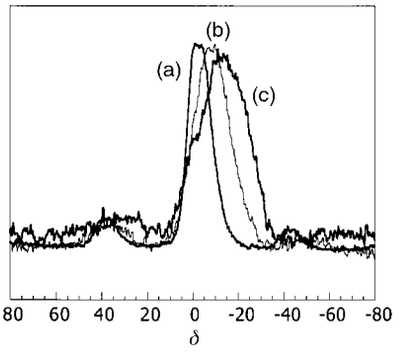

Fig. 6 ^{31}P MAS NMR spectra of (a) surfactant–titanium phosphate mesophase, (b) solvent-extracted and (c) solvent-extracted and calcined (540 °C) mesoporous titanium phosphates (titanium propoxide precursor).

shows the presence of medium–strong acid sites, since 25% of the adsorbed ammonia is removed in the temperature range 400–550 °C. As described above, solvent extracted titanium phosphate evolves structurally and texturally above 300 °C, and thus TPD NH_3 is not an appropriate method for the investigation of the surface acidity of extracted samples. For this reason alternative methods were developed which also allow the determination of the number and strength of acid sites and which are carried out at moderate temperature, 80 °C: two-cycle adsorption of ammonia under static conditions and flow microcalorimetric measurements of ammonia adsorption.

The batch adsorption method involves the two-cycle adsorption of ammonia, in which ammonia doses are sent onto the sample, outgassed under milder conditions (250 °C instead of 550 °C), and the equilibrium pressure measured after every adsorption step. Adsorption at this point is considered to include that of both physi- and chemi-sorbed ammonia, although the adsorption temperature of 80 °C reduces the physisorption phenomenon. At the end of the first adsorption cycle, the sample was then pumped at the adsorption temperature, and a second adsorption cycle performed. Ammonia not removed by pumping at 80 °C is considered to be irreversibly adsorbed, *i.e.* it corresponds to localised chemisorption of single NH_3 molecules on acid sites, and this quantity is derived simply by the difference in adsorption between two adsorption cycles. The two-cycle adsorption of ammonia on solvent extracted and calcined mesoporous titanium phosphates, and the difference curves, are shown in Fig. 8. At the final point of measurement (pressure 38 Torr), the total amount of physi- and chemi-sorbed ammonia is 1955 and 1070 μmol g^{-1} for extracted and calcined samples respectively, of which irreversibly adsorbed ammonia accounts for 900 and 340 μmol g^{-1} respectively. For comparison, under identical conditions of measurement, ZSM-5 in hydrogen form (Si/Al ratio of 15) adsorbs 2450 μmol g^{-1} in total (physi- and chemi-sorbed) and irreversibly adsorbs 1120 μmol g^{-1}. Expressed per unit of surface area, extracted and calcined mesoporous titanium phosphates have a similar surface density of acid sites, 1.66 and 1.5 μmol m^{-2} respectively. The amount of ammonia chemisorbed on the extracted material (900 μmol g^{-1}) is greater than that from the TPD measurement above (711 μmol g^{-1}). Obviously, the discrepancy is ascribed to different experimental conditions under which both tests were carried out. Some changes in structural and textural properties of the material during thermal pre-treatment may account for the decreased surface acidity. For example, the total number of acid sites on the extracted sample, outgassed at 550 °C for 3 h and tested with the use of the two-cycle adsorption method at 80 °C, was decreased to only 275 μmol g^{-1}.

The flow microcalorimetric determination of the pseudo-differential enthalpy (heat) $\Delta_{ads}h$ of ammonia chemisorption at 80 °C appears a more reliable and precise method to determine the strength distribution of surface acid sites. Values of $\Delta_{ads}h$ are the measure of the strength of NH_3 binding to surface acid sites, and thus they allow a quantitative evaluation of the

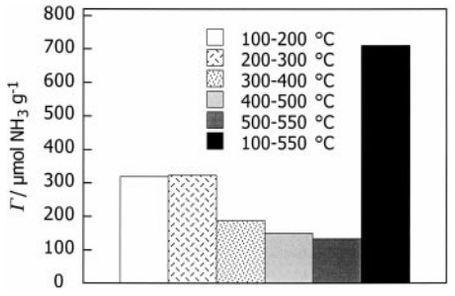

Fig. 7 Thermoprogrammed desorption of ammonia of extracted/calcined mesoporous titanium phosphate (titanium propoxide precursor).

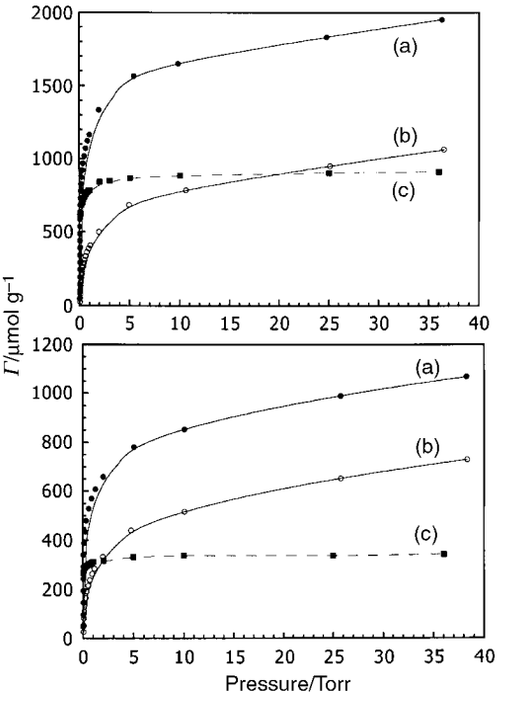

Fig. 8 Two-cycle adsorption of ammonia on (upper panel) solvent-extracted mesoporous titanium phosphate and (lower panel) solvent-extracted and calcined (540 °C) titanium phosphate (titanium propoxide precursor): (a) first adsorption cycle, (b) second adsorption cycle, (c) difference (a)−(b).

strength of such sites. The differential enthalpy curves for extracted and calcined samples are shown in Fig. 9. Each curve exhibits a high initial enthalpy of ammonia chemisorption of *ca.* 120 kJ mol^{-1} after irreversible adsorption of the first ammonia dose (83 μmol g^{-1}, extracted TiP and 62 μmol g^{-1}, calcined TiP). A decrease in the $\Delta_{ads}h$ value is observed with increasing ammonia chemisorption, pointing to the presence of surface sites with lower acid strength. The strength distributions of acid sites in the two samples studied are also presented in Fig. 9. The maximum amount of strong sites showing NH_3 chemisorption enthalpy greater than 80 kJ mol^{-1} is about 30% of the total amount of acid sites on both samples. It is clear that, within each site category, the number of acid sites is diminished during calcination of the extracted sample.

Conclusion

Two different synthetic routes to mesoporous titanium phosphates have been described, and the materials prepared, either using titanium propoxide or *via* modification of a dense titanium phosphate phase precipitated from titanium chloride solution, show distinct textural characteristics. The formation mechanisms operating are different in each case, being possibly a liquid crystal templating type when the former precursor is used, and a folded sheet type in the latter. The surface area of acid–ethanol extracted samples reaches 700 m^2 g^{-1}, and the pore dimensions are uniform and in the mesoporous range; the surface area of materials calcined at 540 °C is around 290 m^2 g^{-1}, and the mesoporous character is retained. Although not well ordered on the long range, XRD indicates and TEM shows local ordering of channel structures. Both extracted and calcined materials are characterised by P(OH) and $P(OH)_2$ groups which decorate the surface, and which are responsible for the high number and high surface density of acid sites. Investigation of the properties of extracted and calcined mesoporous titanium phosphates in fine chemical synthesis and acid catalysis should be of interest, in view of the

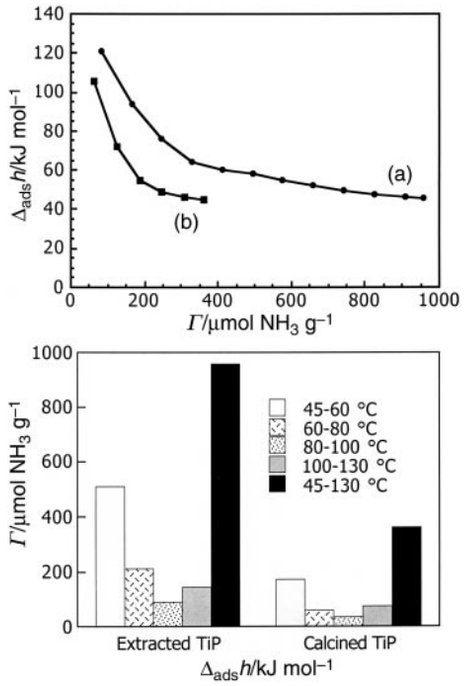

Fig. 9 (Upper panel) Differential enthalpy curves of ammonia chemisorption on mesoporous titanium phosphate (titanium propoxide precursor): (a) solvent-extracted, (b) solvent-extracted and calcined (540 °C) titanium phosphate. (Lower panel) Strength distributions of acid sites.

high surface area and controllable pore size dimensions, and the high number of surface acid sites displayed.

Acknowledgements

This research was supported in part under Brite-EuRam 3 project BRPR-CT97-0560, and funding is acknowledged with thanks.

References

1 J. S. Beck, J. C. Vartuli, W. J. Roth, M. E. Leonowicz, C. T. Kresge, K. D. Schmitt, C. T.-W. Chu, D. H. Olson, E. W. Sheppard, S. B. McCullen, J. B. Higgins and J. C. Schlenker, *J. Am. Chem. Soc.*, 1992, **114**, 10834.
2 A. Corma, M. T. Navarro and J. Perez-Pariente, *J. Chem. Soc., Chem. Commun.*, 1994, 147; P. T. Tanev, M. Chibwe and T. J. Pinnavaia, *Nature*, 1994, **368**, 321.
3 K. M. Reddy, I. Moudrakovski and A. Sayari, *J. Chem. Soc., Chem. Commun.*, 1994, 1059; Z. Luan, J. Xu, H. He, J. Klinowski and L. Kevan, *J. Phys. Chem.*, 1996, **100**, 19595.
4 Z. Y. Yuan, S. Q. Liu, T. H. Chen, J. Z. Wang and H. X. Li, *J. Chem. Soc., Chem. Commun.*, 1995, 973.
5 D. Zhao and D. Goldfarb, *J. Chem. Soc., Chem. Commun.*, 1995, 875.
6 D. J. Jones, J. Jiménez-Jiménez, A. Jiménez-López, P. Maireles-Torres, P. Olivera-Pastor, E. Rodríguez-Castellón and J. Rozière, *Chem. Commun.*, 1997, 431.
7 N. Ulagapan and C. N. R. Rao, *Chem. Commun.*, 1996, 1047.
8 U. Ciesla, D. Demuth, R. Leon, P. Petroff, G. Stucky, K. Unger and F. Schüth, *J. Chem. Soc., Chem. Commun.*, 1994, 1387; Q. Huo, D. Margolese, U. Ciesla, P. Feng, T. E. Gier, P. Sieger, R. Leon, P. Petroff, F. Schüth and G. Stucky, *Nature*, 1994, **368**, 317; Q. Huo, D. Margolese, U. Ciesla, D. G. Demuth, P. Feng, T. E. Gier, P. Sieger, A. Firouzi, B. F. Chmelka, F. Schüth and G. Stucky, *Chem. Mater.*, 1994, **6**, 1176.
9 L. Qi, J. Ma, H. Cheng and A. Zhao, *Langmuir*, 1998, **14**, 2579; K. G. Severin, T. M. Abdel-Fattah and T. J. Pinnavaia, *Chem. Commun.*, 1998, 1471; V. Luca and J. M. Hook, *Chem. Mater.*, 1997, **9**, 2731.
10 A. Stein, M. Fendorf, T. P. Jarvie, K. T. Mueller, A. J. Benezi and T. E. Mallouk, *Chem. Mater.*, 1995, **7**, 304.
11 M. Fröba, O. Muth and A. Reller, *Solid State Ionics*, 1997, **101–103**, 249.
12 A. Sayari and P. Liu, *Microporous Mater.*, 1997, **12**, 149; F. Schüth, *Ber. Bunsenges. Phys. Chem.*, 1995, **99**, 1306.
13 M. Thieme and F. Schüth, *Microporous Mesoporous Mater.*, 1999, **27**, 193.
14 V. F. Stone Jr. and R. J. Davis, *Chem. Mater.*, 1998, **10**, 1468.
15 D. M. Antonelli and J. Y. Ying, *Angew. Chem., Int. Ed. Engl.*, 1995, **34**, 2014.
16 M. S. Wong, D. M. Antonelli and J. Y. Ying, *NanoStruct. Mater.*, 1997, **9**, 165.
17 U. Ciesla, S. Schacht, G. D. Stucky, K. K. Unger and F. Schuth, *Angew. Chem., Int. Ed. Engl.*, 1997, **35**, 541.
18 M. S. Wong and J. Y. Ying, *Chem. Mater.*, 1998, **10**, 2067.
19 U. Ciesla, M. Fröba, G. Stucky and F. Schüth, *Chem. Mater.*, 1999, **11**, 227.
20 D. M. Antonelli, *Microporous Mesoporous Mater.*, 1999, **30**, 315.
21 P. Trens, M. J. Hudson and R. Denoyel, *J. Mater. Chem.*, 1998, **8**, 2147.
22 G. Pacheco, E. Zhao, A. Garcia, A. Sklyarov and J. J. Fripiat, *J. Mater. Chem.*, 1998, **8**, 219; E. Zhao, O. Hernandez, G. Pacheco, S. Hardcastel and J. J. Fripiat, *J. Mater. Chem.*, 1998, **8**, 1635; Neeraj and C. N. R. Rao, *J. Mater. Chem.*, 1998, **8**, 1631.
23 D. Khushalani, G. A. Ozin and A. Kuperman, *J. Mater. Chem.*, 1999, **9**, 1491.
24 A. Bortun, E. Jaimez, R. Llavona, J. R Garcia and J. Rodríguez, *Mater. Res. Bull.*, 1995, **30**, 413.
25 A. Clearfield and J. A. Stynes, *J. Inorg. Nucl. Chem.*, 1964, **26**, 117.
26 A. N. Christensen, E. Krogh Andersen, I. G. Krogh Andersen, G. Alberti, M. Nielsen and M. S. Lehmann, *Acta Chem. Scand.*, 1990, **44**, 865.
27 P. Olivera-Pastor, P. Maireles-Torres, E. Rodríguez-Castellón, A. Jiménez-López, T. Cassagneau, D. J. Jones and J. Rozière, *Chem. Mater.*, 1996, **8**, 1758.
28 D. M. Poojary, A. I. Bortun, L. N. Bortun and A. Clearfield, *J. Solid State Chem.*, 1997, **132**, 213; A. I. Bortun, L. Bortun, A. Clearfield, M. A. Villa-García, J. R. García and J. Rodríguez, *J. Mater. Res.*, 1996, **10**, 2490; Y. Bereznitski, M. Jaroniec, A. I. Bortun, D. M. Poojary and A. Clearfield, *J. Colloid Interface Sci.*, 1997, **191**, 442; A. I. Bortun, S. E. Khainakov, L. N. Bortun, D. M. Poojary, J. Rodríguez, J. R. García and A. Clearfield, *Chem. Mater.*, 1997, **9**, 1805.
29 S. Ekambaram and S. C. Sevov, *Angew. Chem., Int. Ed.*, 1999, **38**, 372.
30 T. Doi and T. Miyake, *Chem. Commun.*, 1996, 1635.
31 S. Inagaki, Y. Fukushima and K. Kuroda, *Stud. Surf. Sci. Catal.*, 1994, **84**, 125; S. Inagaki, Y. Sakamoto and O. Terasaki, *Chem. Mater.*, 1996, **8**, 2089.
32 G. Alberti, M. Casciola, F. Marmottini and R. Vivani, *J. Porous Mater.*, 1999, **6**, 299.
33 J. Jiménez-Jiménez, P. Maireles-Torres, P. Olivera-Pastor, E. Rodriguez-Castellón, A. Jiménez-López, D. J. Jones and J. Rozière, *Adv. Mater.*, 1998, **10**, 812.
34 R. W. Cranston and F. A. Inkley, *Adv. Catal.*, 1957, **9**, 143.
35 M. J. Meziani, J. Zajac, D. J. Jones, S. Partyka, J. Rozière and A. Auroux, *Langmuir*, 2000, **16**, 2262.
36 A. J. Groszek, *Thermochim. Acta*, 1998, **312**, 133.
37 V. Alfredsson, M. Keung, A. Monnier, G. D. Stucky, K. K. Unger and F. Schüth, *J. Chem. Soc., Chem. Commun.*, 1994, 921.
38 J. Feng, Q. Huo, P. M. Petroff and G. D. Stucky, *Appl. Phys. Lett.*, 1997, **71**, 620.
39 M. J. Hudson and A. D. Workman, *J. Mater. Chem.*, 1991, **1**, 375.
40 H. Nakayama, T. Eguchi, N. Nakamura, S. Yamaguchi, M. Danjyo and M. Tsuhako, *J. Mater. Chem.*, 1997, **7**, 1063.
41 A. I. Bortun, S. B. Randarevich and G. A. Malinovskii, *Russ. J. Inorg. Chem.*, 1989, **34**, 1776.
42 Y. J. Li and M. S. Whittingham, *Solid State Ionics*, 1993, **63**, 391.
43 D. J. MacLachlan and K. R. Morgan, *J. Phys. Chem.*, 1990, **94**, 7656; D. J. MacLachlan and K. R. Morgan, *J. Phys. Chem.*, 1992, **96**, 3458.
44 G. Busca, V. Lorenzelli, P. Galli, A. La Ginestra and P. Patrono, *J. Chem. Soc., Faraday Trans. 1*, 1987, **83**, 853.